Communication: Predictive partial linearized path integral simulation of condensed phase electron transfer dynamics

Pengfei Huo, Thomas F. Miller, and David F. Coker

View Online   Export Citation   CrossMark

Communication: Predictive partial linearized path integral simulation of condensed phase electron transfer dynamics

Pengfei Huo,[1,a)] Thomas F. Miller III,[1,b)] and David F. Coker[2,c)]

[1]*Division of Chemistry and Chemical Engineering, California Institute of Technology, Pasadena, California 91125, USA*

[2]*Department of Chemistry, Boston University, 590 Commonwealth Avenue, Boston, Massachusetts 02215, USA*

A partial linearized path integral approach is used to calculate the condensed phase electron transfer (ET) rate by directly evaluating the flux-flux/flux-side quantum time correlation functions. We demonstrate for a simple ET model that this approach can reliably capture the transition between non-adiabatic and adiabatic regimes as the electronic coupling is varied, while other commonly used semi-classical methods are less accurate over the broad range of electronic couplings considered. Further, we show that the approach reliably recovers the Marcus turnover as a function of thermodynamic driving force, giving highly accurate rates over four orders of magnitude from the normal to the inverted regimes. We also demonstrate that the approach yields accurate rate estimates over five orders of magnitude of inverse temperature. Finally, the approach outlined here accurately captures the electronic coherence in the flux-flux correlation function that is responsible for the decreased rate in the inverted regime. © *2013 AIP Publishing LLC*. [http://dx.doi.org/10.1063/1.4826163]

Electron transfer (ET) reactions are essential in chemical and biological process. For a system with classical nuclei, the non-adiabatic Marcus ET theory gives the thermal rate constant as[1,2]

$$k_{MT} = \frac{\Delta^2}{\hbar} \sqrt{\frac{\beta\pi}{\lambda}} \exp\left[-\beta \frac{(\epsilon - \lambda)^2}{4\lambda}\right] \qquad (1)$$

with ϵ the free energy difference between donor and acceptor states, λ the solvent reorganization energy, Δ the non-adiabatic electronic coupling, $\beta = 1/k_B T$ and the activation free energy is $G^\ddagger = (\epsilon - \lambda)^2/4\lambda$. Despite its predictive success, trajectory based methods that incorporate a quantum electronic description and semi-classical treatment of solvent fluctuations are desirable for explicit simulation of ET in complex systems.[3–5]

Methods for simulating condensed phase non-adiabatic processes include Ehrenfest or semi-classical approaches based on the initial value representation (SC-IVR).[6,7] In particular, linearized approximations (LSC-IVR)[8–11] provide trajectory-based computation of thermal reaction rates. Ehrenfest methods encounter problems in the electronically adiabatic regime,[12] while LSC-IVR methods[8] are less reliable in the non-adiabatic limit.[10,11]

Imaginary-time path-integral methods, such as semi-classical instanton theory (SCI)[13–15] and ring polymer molecular dynamics (RPMD)[16,17] include nuclear tunneling effects. These can accurately treat the ET rate in the normal regime,[14,18,19] but fail in the Marcus inverted region due to breakdown of SCI theory as applied to deep tunneling between asymmetric wells.[18] Nevertheless, developments in the

methodology and analysis of RPMD show promise in addressing this issue.[20–23]

Trajectory surface hopping (SH) techniques have also been explored in the context of ET rate constant calculations.[4] Recent studies have demonstrated the success of the SH method for calculating the ET rate in various parameter regimes.[12,24] However, these studies show implementation dependence[12,24] related to treatment of electronic decoherence,[24] or ambiguous choice of estimator for state populations.[12]

Recently, two of us presented a partial linearized semi-classical approach to propagate the density matrix (PLDM).[25] Rather than linearizing the dynamics of all degrees of freedom (DOF) as with LSC-IVR, PLDM only linearizes in the nuclear DOF, explicitly keeping forward and backward paths of the electronic DOF. This method can be viewed as a partial forward-backward (FB) path integral approach.[7] An important feature of PLDM dynamics observed numerically in model problems[25,26] is that it not only accurately captures the short time coherent behavior, but also relaxes to a reliable description of thermal equilibrium in the quantum subsystem state populations. In fact, it has been recently demonstrated[27] that iterative implementation of PLDM[26] is equivalent to the full solution of the mixed quantum-classical Liouville (MQCL) equation,[28] which is exact for spin-boson problems[29] and in general the stationary solution of the MQCL equation agrees to $\mathcal{O}(\hbar)$ with the exact quantum equilibrium density.[30] This is important as reliable results for transport properties are sensitive to accurate relaxation to thermal equilibrium. Neither LSC-IVR nor Ehrenfest dynamics recover thermal equilibrium state populations at long time due to their approximate mean field treatment, though surface hopping methods seem to describe thermalization accurately in model studies.[31] These features of the PLDM

a)Electronic mail: pengfhuo@caltech.edu
b)Electronic mail: tfm@caltech.edu
c)Electronic mail: coker@bu.edu

approach suggest that it may provide better ET rates than other trajectory based methods in various regimes. We explore this proposal in the current communication.

The exact expressions for the thermal rate constant, equivalently written as the integral of the flux-flux correlation function, $C_{ff}(t)$, or the long-time limit of the flux-side correlation function, $C_{fs}(t)$ are[32–35]

$$k = Q_r^{-1} \int_0^\infty \text{Re}[C_{ff}(t)]dt = Q_r^{-1} \lim_{t\to\infty} \text{Re}[C_{fs}(t)], \quad (2)$$

where $C_{fs}(t) = \text{Tr}[\hat{\rho}\hat{F}e^{i\hat{H}t/\hbar}\hat{h}e^{-i\hat{H}t/\hbar}]$ and $C_{ff}(t) = \text{Tr}[\hat{\rho}\hat{F}e^{i\hat{H}t/\hbar}\hat{F}e^{-i\hat{H}t/\hbar}]$. Here $\hat{\rho} = e^{-\beta\hat{H}}$, $\hat{H}$ is the total hamiltonian operator and $Q_r = \text{Tr}[\hat{\rho}\hat{h}]$, is the reactant partition function. The side operator, $\hat{h}$, represents the dividing surface that distinguishes between reactant and product regions, and $\hat{F} = i/\hbar[\hat{H}, \hat{h}]$ is the flux operator.

The real-time correlation function of operators $\hat{A}$ and $\hat{B}$ with discrete electronic states and continuous environmental variables is

$$C_{AB}(t) = \langle\hat{A}\hat{B}(t)\rangle = \text{Tr}[\hat{\rho}\hat{A}e^{\frac{i}{\hbar}\hat{H}t}\hat{B}e^{-\frac{i}{\hbar}\hat{H}t}]$$

$$= \sum_{n_0n_t,n_0'n_t'}\int dR_0dR_NdR_0'dR_N'\langle R_0n_0|\hat{\rho}\hat{A}|R_0'n_0'\rangle$$

$$\times\langle R_0'n_0'|e^{\frac{i}{\hbar}\hat{H}t}|R_N'n_t'\rangle B_{n_t'n_t}\langle R_Nn_t|e^{-\frac{i}{\hbar}\hat{H}t}|R_0n_0\rangle,$$

$$(3)$$

where $B_{n_t'n_t} = \langle n_t'R_N'|\hat{B}|n_tR_N\rangle$. We replace the evolution of the discrete electronic subsystem exactly by the continuous dynamics of a system of fictitious mapping harmonic oscillators,[37] thus putting the description of the evolution of the nuclear and electronic DOF on the same footing. The quantum state operators map to the continuous variables of the harmonic oscillators as: $|\beta\rangle\langle\alpha| \to \hat{a}_\beta^\dagger\hat{a}_\alpha$, where $\hat{a}_\alpha = \frac{1}{\sqrt{2\hbar}}(\hat{q}_\alpha - i\hat{p}_\alpha)$. We transform the forward and backward nuclear DOF, R and R', to the mean $\bar{R} = (R + R')/2$ and difference $Z = R - R'$ variables, and linearize the combined forward-backward propagator in Z.[8,11,38] Keeping all orders in the electronic DOF, we express them using mapping variables in the coherent state representation,[25,38] giving

$$C_{AB}(t) = \sum_{n_0,n_t,n_0'n_t'}\int d\bar{R}_0dq_0dp_0dq_0'dp_0'G_0G_0'$$

$$\times\int\prod_{k=1}^N d\bar{R}_k\frac{d\bar{P}_k}{2\pi\hbar}T_{[n0,nt]}T_{[nt',n0']}'$$

$$\times(\hat{\rho}\hat{A})_W^{n_0,n_0'}(\bar{R}_0, \bar{P}_1)[\hat{B}_W^{n_t',n_t}]^*(\bar{R}_N, \bar{P}_N)$$

$$\times\prod_{k=1}^{N-1}\delta\left(\frac{\bar{P}_{k+1} - \bar{P}_k}{\epsilon} - F_k\right)\prod_{k=1}^N\delta\left(\frac{\bar{P}_k}{M} - \frac{\bar{R}_k - \bar{R}_{k-1}}{\epsilon}\right).$$

$$(4)$$

This result gives a generalized method to computing thermal time correlation functions. Here, $G_0 = e^{-\frac{1}{2}\sum_\beta(q_{\beta0}^2 + p_{\beta0}^2)}$ and $G_0' = e^{-\frac{1}{2}\sum_{\beta'}(q_{\beta'0}^2 + p_{\beta'0}^2)}$ provide the initial distributions for the forward and backward mapping vari-

ables, and $T_{[n0,nt]} = \frac{1}{4}(q_{n_t} + ip_{n_t})(q_{n_0} - ip_{n_0})$, and $T_{[nt',n0']}' = \frac{1}{4}(q_{n_t'}' - ip_{n_t'}')(q_{n_0'}' + ip_{n_0'}')$ are the electronic transition amplitudes. The partial Wigner transform $(\hat{\rho}\hat{A})_W^{n_0,n_0'} = \int dZ_0\langle\bar{R}_0 + \frac{Z_0}{2}n_0|\hat{\rho}\hat{A}|\bar{R}_0 - \frac{Z_0}{2}n_0'\rangle e^{-\frac{i}{\hbar}\bar{P}_1Z_0}$ provides trajectory initial conditions[39] and $[\hat{B}_W^{n_t',n_t}]^*(\bar{R}_N, \bar{P}_N) = \int dZ_N\langle\bar{R}_N - \frac{Z_N}{2}n_t'|\hat{B}|\bar{R}_N + \frac{Z_N}{2}n_t\rangle e^{\frac{i}{\hbar}\bar{P}_NZ_N}$. The PLDM equations of motion are[25]

$$\dot{q}_{n_t} = \partial h_m^{cl}(\bar{R}_t)/\partial p_{n_t}; \dot{p}_{n_t} = -\partial h_m^{cl}(\bar{R}_t)/\partial q_{n_t},$$

$$(5)$$

$$F_k = -\frac{1}{2}\nabla_{\bar{R}_k}\left[h_m^{cl}(\bar{R}_k, p_k, q_k) + h_m^{cl}(\bar{R}_k, p_k', q_k')\right],$$

where $h_m^{cl}(R, p, q) = \frac{1}{2}\sum_\alpha h_{\alpha\alpha}(R)(p_\alpha^2 + q_\alpha^2) + \frac{1}{2}\sum_{\gamma\neq\alpha}\times h_{\gamma\alpha}(R)(p_\gamma p_\alpha + q_\gamma q_\alpha)$.[25,38] These PLDM equations can be put into hamiltonian form by canonical transformation, defining the tilde variables by dividing all mapping DOF by $\sqrt{2}$ giving $H_{tot}(\bar{P}, \bar{R}, \tilde{p}, \tilde{q}, \tilde{p}', \tilde{q}') = \bar{P}^2/2M + h_m^{cl}(\bar{R}, \tilde{p}, \tilde{q}) + h_m^{cl}(\bar{R}, \tilde{p}', \tilde{q}')$.[27]

Our model ET hamiltonian has the form

$$\hat{H} = \frac{1}{2}\epsilon\sigma_z + \Delta\sigma_x + \frac{P^2}{2} + \frac{\Omega^2Q^2}{2} + C_sQ\sigma_z + \hat{H}_{s-b}, \quad (6)$$

where $\hat{H}_{s-b} = \sum_i\frac{1}{2}[p_i^2 + \omega_i^2(q_i + c_iQ/\omega_i^2)^2]$, $\sigma_z = |1\rangle\langle1| - |2\rangle\langle2|$, $\sigma_x = |1\rangle\langle2| + |2\rangle\langle1|$, and $|1\rangle$ and $|2\rangle$ specify electron donor and acceptor state, respectively. A collective solvent coordinate Q with frequency Ω is linearly coupled to the electronic subsystem with strength $C_s = \sqrt{\lambda\Omega^2/2}$.[24] The Q coordinate is also linearly coupled to a set of dissipative bath DOF, with coupling strengths c_i, determined from the spectral density $j(\omega) = \frac{\pi}{2}\sum_i(c_i^2/\omega_i)\delta(\omega - \omega_i) = \eta\omega\exp^{-\omega/\omega_c}$; here, η is the solvent friction parameter and ω_c is the ohmic bath cutoff frequency.[40,41] The model parameters (in atomic units) for all calculations are as used in Ref. 24, with $\Omega = 3.5 \times 10^{-4}$, $\lambda = 2.39 \times 10^{-2}$, $\eta = 1.49 \times 10^{-5}$,[42] $\omega_c = \Omega$, $k_BT = 9.5 \times 10^{-4}$, and $\Delta = 5 \times 10^{-5}$.

For the ET model considered, we employ a convenient and widely used dividing surface[8,18,43] such that $\hat{h} = |2\rangle\langle2|$, so $\hat{F} = i\Delta/\hbar[|1\rangle\langle2| - |2\rangle\langle1|]$. Initial conditions from the Wigner transformed thermal flux operator $(e^{-\beta\hat{H}}\hat{F})_W$ could be sampled exactly[44] or using the approximate expression[8] $(e^{-\beta\hat{H}}\hat{F})_W \approx (e^{-\beta\hat{H}_b})_W(\hat{F})_W$. However, formulation of the rate constant in this way leads to significant increase in the oscillations of $C_{ff}(t)$ with increasing driving force and results in considerable numerical difficulty converging the rates in the inverted regime.[45] An alternative perturbative expansion[46] of $e^{-\beta\hat{H}}$ gives numerically favorable evaluation of the rate in both normal and inverted regimes. Here the thermal flux operator used is[10,11] $(e^{-\beta\hat{H}_{11}})_W(\hat{F})_W$, and we sample initial collective DOF from $(e^{-\beta\hat{H}_{11}})_W = \tanh(\frac{\beta\Omega}{2})\exp[-\frac{\tanh(\beta\Omega/2)}{\Omega}(\bar{P}^2 + \Omega^2(\bar{Q} + \frac{C_s}{\Omega^2})^2)]$.[12] The supplementary materials[45] detail numerical convergence.

Figure 1 compares various approximate trajectory-based methods for computing the ET rate constant in the symmetric case ($\epsilon = 0$). The electronic coupling, Δ, is varied over many orders of magnitude and demonstrates that the rate calculated from the approximate PLDM result in Eq. (4) accurately recovers the crossover from the non-adiabatic regime at weak electronic coupling to the adiabatic regime for strong
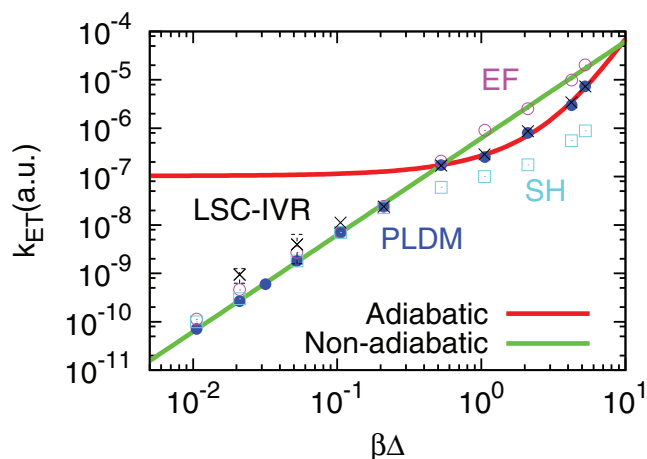
FIG. 1. PLDM computed ET rate (blue points) as a function of $\beta\Delta$, for $\epsilon = 0$ (see text for other parameters). The non-adiabatic rate (green) is obtained from Eq. (1). The adiabatic rate (red) is $k_{ad} = (\Omega/2\pi)\exp[-\beta G^{\ddagger}_{ad}]$, where Ω is the frequency of the reactant well, and $G^{\ddagger}_{ad}$ is the energy difference between the minimum and the barrier of the ground adiabatic state.[2] Rates obtained using Ehrenfest (magenta circles); surface hopping (cyan boxes); and LSC-IVR (black crosses, with worst error bars) are compared.

coupling.[45] The results of other methods displayed are less accurate across this broad range of coupling. The LSC-IVR approach,[8] while providing accurate results in the strong coupling adiabatic limit, deviates significantly from the analytic result in the non-adiabatic regime giving rates that are nearly an order of magnitude too large.[10, 11] On the other hand, Ehrenfest and SH dynamics (as implemented in Ref. 12), which generally perform better in the non-adiabatic limit, deviate significantly, in different ways, from the adiabatic rate expression in the strong electronic coupling regime. The ET rates calculated using the state resolved instanton approach,[14] the imaginary-time flux-flux correlation function method,[36] and RPMD[19] also accurately capture the transition between the adiabatic and non-adiabatic limits for symmetric electron transfer despite the break down in the inverted regime for this class of methods mentioned above.[18] As a stringent test, we next explore the PLDM rate constant as a function of driving force.

Figure 2(a) compares the PLDM rate[45] with k_{MT} from Eq. (1). Under ambient conditions, k_{MT} yields the golden rule rate. The PLDM approach quantitatively captures the Marcus turn over across the entire range of driving force, giving predictive capability over at least four orders of magnitude. Figure 2(b) shows that PLDM calculations recover the inverse temperature dependence of the ET rate over five orders of magnitude and across a wide range of driving force in the inverted region. Marcus theory, which assumes classical nuclei, starts to deviate from the quantum golden rule rate[8, 11, 33] at low temperature, but the PLDM results agree closely with the golden rule rate due to the explicit inclusion of zero point energy through sampling the initial Wigner distribution. As noted earlier, if PLDM is implemented iteratively the approach is equivalent to the full solution of the mixed quantum classical Liouville equation.[27] Without iteration the classical-like nuclear dynamics cannot in general guarantee maintenance of the correct distribution of zero-point energy in the
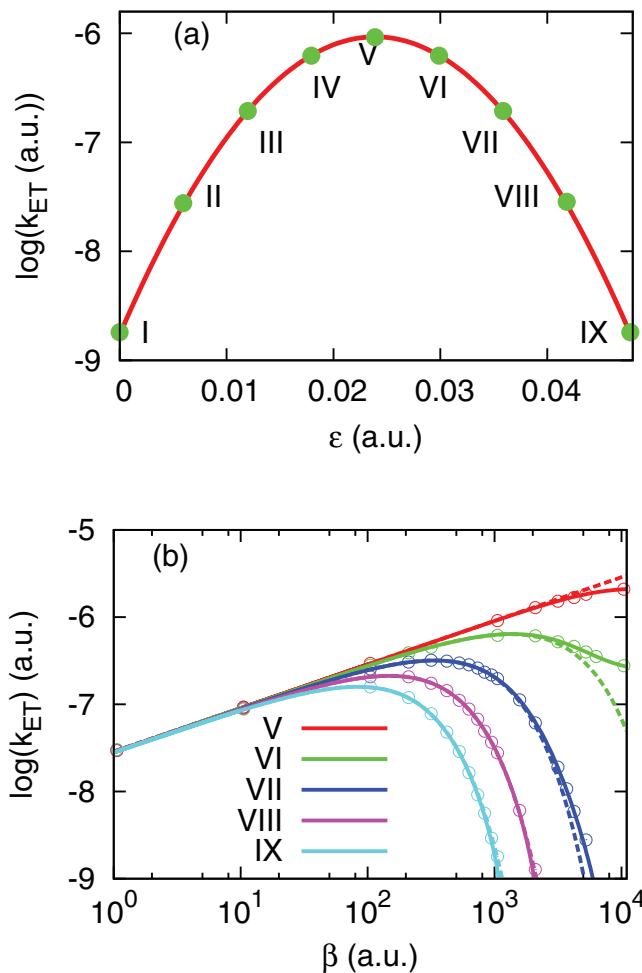

FIG. 2. (a) Rate calculated from PLDM flux-side correlation function (green dots) compare to k_{MT} (solid red curve) as a function of ϵ at T = 300 K for: (I) $\epsilon = 0$; (II) 0.25λ; (III) 0.5λ; (IV) 0.75λ; (V) λ; (VI) 1.25λ; (VII) 1.5λ; (VIII) 1.75λ; and (IX) 2λ. Cases I–IV – normal regime, case V – activationless, and case VI–IX – inverted regime. (b) PLDM computed ET rates (open circles) as a function of inverse temperature β for various inverted regime ϵ. Dashed curves from Eq. (1) and solid curves are golden rule rates.[8, 11, 33]

system (the zero-point energy flow problem[47, 48]). However, since the ET rate constant is determined by short time dynamics, the initial Wigner distribution can maintain a reliable distribution of zero-point energy for long enough to give accurate rate constant estimates.

Figure 3(a) presents results for $C_{fs}(t)$ in the inverted regime using PLDM propagation with initial conditions sampled from $(e^{-\beta\hat{H}_{11}})_W(\hat{F})_W$. Rate estimates are obtained from the plateau values achieved very rapidly after recrossing dynamics. Figure 3(b) shows excellent agreement between the PLDM flux-flux correlation function computed under these conditions and the analytical golden rule expression.[45] For comparison with alternative approximate initial condition calculations, $(e^{-\beta\hat{H}_b})_W(\hat{F})_W$, see the supplementary material.[45]

Finally, we note that the PLDM approach[25] is successful because it accurately accounts for electronic interference effects. Our findings also suggest that the approach is reliable even without short time iteration since the ET rates are determined by short time relaxation and recrossing dynamics.[45]
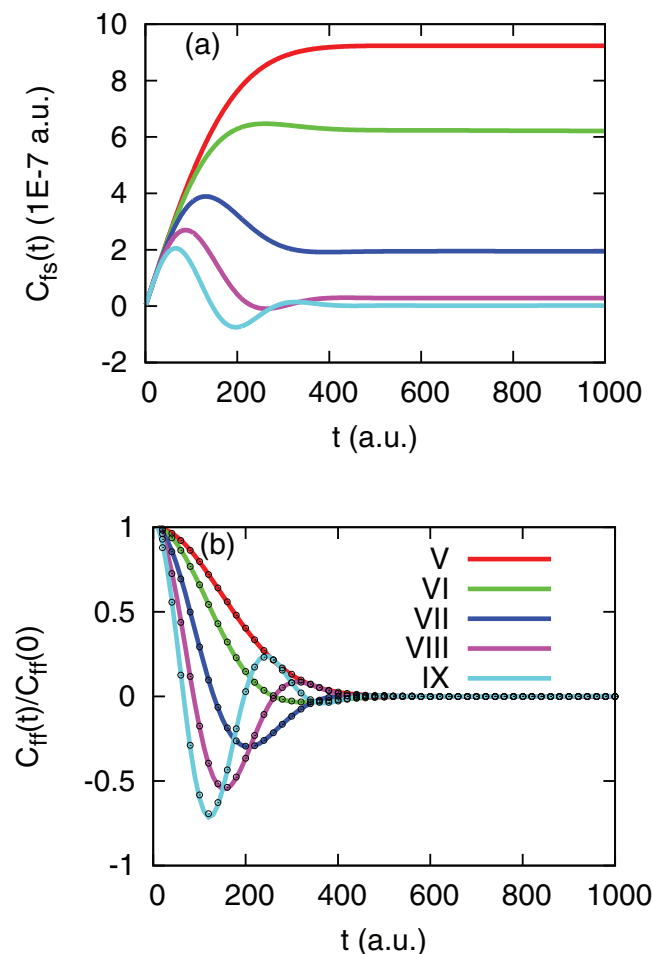
FIG. 3. (a) Inverted regime correlation functions with initial condition $(e^{-\beta \hat{H}_{11}})_W (\hat{F})_W$. Panel (b) compares with $e^{-\lambda t^2/\hbar^2 \beta} \cos[(\epsilon - \lambda)t/\hbar]$ (open circles).[45]

[1] R. A. Marcus, J. Chem. Phys. **24**, 966 (1956).
[2] R. A. Marcus, Annu. Rev. Phys. Chem. **15**, 155 (1964).
[3] S. Shin and H. Metiu, J. Chem. Phys. **102**, 9285 (1995).
[4] R. E. Cline, Jr. and P. G. Wolynes, J. Chem. Phys. **86**, 3836 (1987).
[5] J. E. Straub, M. Borkovec, and B. J. Berne, J. Chem. Phys. **89**, 4833 (1988).
[6] Y. Zhao and W. Liang, Front. Chem. China **5**, 423 (2010).
[7] H. Wang, M. Thoss, and W. H. Miller, J. Chem. Phys. **112**, 47 (2000).
[8] H. Wang, X. Song, D. Chandler, and W. H. Miller, J. Chem. Phys. **110**, 4828 (1999).
[9] H. Wang, X. Sun, and W. H. Miller, J. Chem. Phys. **108**, 9726 (1998).
[10] E. Rabani, S. A. Egorov, and B. J. Berne, J. Phys. Chem. A **103**, 9539 (1999).
[11] Q. Shi and E. Geva, J. Phys. Chem. A **108**, 6109 (2004).
[12] W. Xie, S. Bai, L. Zhu, and Q. Shi, J. Phys. Chem. A **117**, 6196 (2013).
[13] A. O. Caldeira and A. J. Leggett, Ann. Phys. **149**, 374 (1983); W. H. Miller, J. Chem. Phys. **62**, 1899 (1975).
[14] J. Cao and G. A. Voth, J. Chem. Phys. **106**, 1769 (1997).
[15] S. Jang and J. Cao, J. Chem. Phys. **114**, 9959 (2001).
[16] I. R. Craig and D. E. Manolopoulos, J. Chem. Phys. **122**, 084106 (2005); **123**, 034102 (2005).
[17] S. Habershon, D. E. Manolopoulos, T. E. Markland, and T. F. Miller III, Annu. Rev. Phys. Chem. **64**, 387 (2013).
[18] A. R. Menzeleev, N. Ananth, and T. F. Miller III, J. Chem. Phys. **135**, 074106 (2011).
[19] J. S. Kretchmer and T. F. Miller III, J. Chem. Phys. **138**, 134109 (2013).
[20] A. R. Menzeleev, F. Bell, and T. F. Miller III, "Kinetically constrained ring polymer molecular dynamics for non-adiabatic chemical reactions" (unpublished).
[21] P. Shushkov, J. Phys. Chem. **138**, 224102 (2013).
[22] J. O. Richardson and M. Thoss, J. Chem. Phys. **139**, 031102 (2013).
[23] N. Ananth, J. Chem. Phys. **139**, 124102 (2013).
[24] B. R. Landry and J. E. Subotnik, J. Chem. Phys. **135**, 191101 (2011); **137**, 22A513 (2012).
[25] P. Huo and D. F. Coker, J. Chem. Phys. **135**, 201101 (2011).
[26] P. Huo and D. F. Coker, J. Chem. Phys. **137**, 22A535 (2012).
[27] C.-Y. Hsieh and R. Kapral, J. Chem. Phys. **138**, 134110 (2013).
[28] R. Kapral and G. Ciccotti, J. Chem. Phys. **110**, 8919 (1999).
[29] D. MacKernan, G. Ciccotti, and R. Kapral, J. Chem. Phys. **116**, 2346 (2002).
[30] S. Nielsen, G. Ciccotti, and R. Kapral, J. Chem. Phys. **115**, 5805 (2001).
[31] J. R. Schmidt, P. V. Parandekar, and J. C. Tully, J. Chem. Phys. **129**, 044104 (2008); P. V. Parandekar and J. C. Tully, J. Chem. Theory Comput. **2**, 229 (2006).
[32] W. H. Miller, S. D. Schwartz, and J. W. Tromp, J. Chem. Phys. **79**, 4889 (1983).
[33] S. A. Egorov, E. Rabani, and B. J. Berne, J. Chem. Phys. **110**, 5238 (1999).
[34] H. Kim and R. Kapral, J. Chem. Phys. **123**, 194108 (2005).
[35] P. Shushkov, R. Li, and J. C. Tully, J. Chem. Phys. **137**, 22A549 (2012).
[36] S. Yang and J. Cao, J. Chem. Phys. **122**, 094108 (2005).
[37] H. D. Meyer and W. H. Miller, J. Chem. Phys. **70**, 3214 (1979); G. Stock and M. Thoss, Phys. Rev. Lett. **78**, 578 (1997).
[38] S. Bonella, D. Montemayor, and D. F. Coker, Proc. Natl. Acad. Sci. U.S.A. **102**, 6715 (2005).
[39] Q. Shi and E. Geva, J. Phys. Chem. A **107**, 9059 (2003).
[40] In the limit of $\omega_c \to \infty$ (here we found $\omega_c = \Omega$ is sufficient[18]), Eq. (6) can be re-expressed as a spin-boson model[41] with a brownian spectral density: $j_{br}(\omega) = \lambda_0 \Omega^2 \eta \omega/[(\omega^2 - \Omega^2)^2 + \eta^2 \omega^2]$, and $\lambda = 1/\pi \int_0^\infty d\omega j_{br}(\omega)/\omega = \lambda_0/2$. As a consistency check we verified that identical results are obtained with either model.
[41] A. Garg, J. N. Onuchic, and V. Ambegaokar, J. Chem. Phys. **83**, 4491 (1985).
[42] Here we choose the friction parameter in the range where the rate is invariant to changes of η (plateau region) according to Ref. 43.
[43] M. Topaler and N. Makri, J. Phys. Chem. **100**, 4430 (1996).
[44] N. Ananth and T. F. Miller III, J. Chem. Phys. **133**, 234103 (2010).
[45] See supplementary material at http://dx.doi.org/10.1063/1.4826163 for calculation details, approximate correlation functions, initial distribution sampling, and analytic limits including Zusman's model.
[46] G. A. Voth, D. Chandler, and W. H. Miller, J. Phys. Chem. **93**, 7009 (1989).
[47] U. Müller and G. Stock, J. Chem. Phys. **111**, 77 (1999).
[48] G. Stock and U. Müller, J. Chem. Phys. **111**, 65 (1999).